Pergamon

www.elsevier.com/locate/actaastro

*Acta Astronautica* Vol. 50, No. 3, pp. 159–166, 2002

PII: S0094-5765(01)00151-5

0094-5765/02/$ - see front matter

# DESIGN OF THE RADIATION SHIELDING FOR A MICROSATELLITE†

GIOVANNI B. PALMERINI‡ and FRANCESCO PIZZIRANI

Scuola di Ingegneria Aerospaziale, Universitá degli Studi di Roma "la Sapienza",
18, via Eudossiana - 00184 Roma, Italy

*(Received 25 August 1999)*

**Abstract**—This paper aims to provide a detailed description of the problems concerning the radiation environment faced while designing a microsatellite at the University of Rome. Although main features of the microsatellite, as well as the environment characteristics expected in candidate orbits are detailed, emphasis is given to expose a generally appropriate procedure for this class of spacecraft. The sector analysis is carried on, and a simple qualitative way to point out critical areas of shielding is shown. The risk concerning the specific devices is assessed, both for total ionization dose and single event upset. The effect of the spot shielding on the most sensitive devices is considered, in order to mitigate SEE occurrence. © 2002 International Astronautical Federation. Published by Elsevier Science Ltd. All rights reserved

## 1. INTRODUCTION

Radiation effects have become a problem for satellites since late seventies. The concern for the problem increased with the lowest critical charge of the new, largely integrated, electronic devices. Quite a large interest has been devoted to this topic, and a general comprehension is now available, ranging from the occurrence of single event effects (SEE) to the long-term maximum amount of radiation received and the related Total Ionization Dose (TID) [1]. Loss of component functionality, data processing anomalies or, possibly, the failure of the mission, due to badly modified code execution, are the undesired consequences of these phenomena.

Current technologies are actually able to provide a solution, as an example by taking advantage from especially designed radiation hardened devices (mitigating both SEE and TID constraints), or by using error detection and correction (EDAC) units.

Unfortunately, these countermeasures do not match anytime with the mission requirements. Especially low-cost missions, now strongly popular with the present trend towards microsatellites, face serious obstacles. Budget constraints and difficult availability [2] limit the expensive rad-hard devices, while several factors, and above all the search for simplest solutions, play against EDAC units. Their introduction, if not quite expensive as the fault tolerant devices, usually requires a time-expensive, careful examination of the memories and processing units, and quite an accurate design of their interfaces: therefore, using EDAC devices (that imply some kind of redundancy) might have to be limited.

Shielding sensitive components can be a classical but valuable solution. Design will be strongly dependent on the chosen orbit. Protection will be devoted as much as possible to the "pre-existing" items capable to work as shields, as the structure or the batteries, prior to the inclusion of additional lids. Careful evaluation of these "free" shields as well as a cost-effective design of the new ones are then mandatory [3], both in terms of the material and of correct placing. The penalty function to be minimized will be of course the mass at launch.

This paper aims to introduce the experience obtained in designing the microsatellite now under development at the University of Rome [4]. As a low-cost educational project, the protection from radiation effects is a major issue for our program, outlined from the desire to fly devices as much as possible off-the-shelf or recently developed, and is not yet qualified for space. The steps followed in the design, with the software tools developed and

†Paper IAF-97-I.3.07 presented at the 48th International Astronautical Congress, October 6–10, 1997, Turin, Italy

‡Corresponding author. Tel.: +39-06-4458-5334; fax: +39-06-4458-5952.

*E-mail address:* gp-gauss@caspur.it (G.B. Palmerini).

used, are presented; identification of critical components is carried on; the environmental risk of the low orbit chosen for the microsatellite is assessed. The final goal is to outline how the material selection, the structure shaping and the components placing will contribute to reduce the undesired radiation effects.

## 2. THE UNISAT MICROSATELLITE

The UNISAT program is a project developed at the Scuola di Ingegneria Aerospaziale of the University of Rome "*la Sapienza*", in a joint effort with other Italian universities. This activity has a strong educational commitment, enjoying a cooperation to similar programs worldwide: preliminary design of the satellite resulted from the experience of the team-members at the Stanford University, Space Systems Design Lab, where the SQUIRT microsatellites is being designed and built.

The UNISAT microsatellite (Fig. 1) is intended to be a multi-purpose bus, able to carry on a wide set of experiments with none or minimal changes. Indeed, the configuration is modular, with a sequence of trays superimposed. Modular shape allows for a quick separation of different subsystems, making manufacturing and testing easier.

Current configuration of the microsatellite presents a prismatic shape with an octagonal base. The side of the octagon is 15 cm, while the height is 25 cm in the basic model. The structure is made by aluminum skin/aluminum honeycomb sandwich panels. Four steel bars join the different planes, blocked out of the bottom and top trays by eight bolts, "packing" the microsatellite. Sixteen aluminum spacers, four in each floor, inserted around the steel bars, provide the distance between the trays.

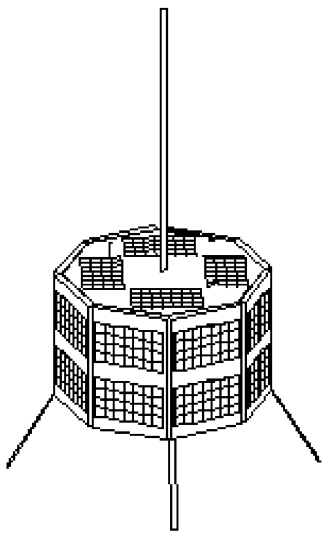

Fig. 1. A sketch of the UNISAT microsatellite.

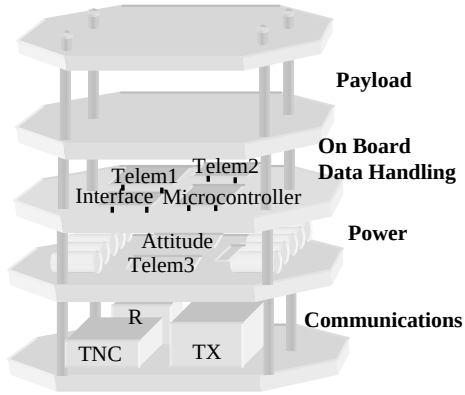


Fig. 2. UNISAT internal architecture.

In the configuration (as in July 1997) examined in the following, four compartments are provided (Fig. 2). The lowest houses the transmitter, the receiver and the terminal node controller (TNC). The second compartment holds the batteries and the power conditioning devices, the board with the electronics to drive the magnetic coils for the attitude control, and a telemetry board for power and attitude monitoring. Third floor is for the on-board data handling, with the microcontroller, the operational software and data memories, the interfaces to all the systems, and two telemetry boards for panel-related current and temperature measures. Top compartment, which height can be varied according to the instruments characteristics, is reserved for the payload.

The shielding is mainly provided by the side panels, the solar panels mounted on them, the trays, the batteries and the boxes. Their diameter is not negligible, and the spacers will also be taken into account in the following analysis of the shielding offered by the structure.

## 3. EVALUATION OF THE EXPOSURE TO RADIATIONS

### *3.1. Sector analysis*

The method pursued for the shielding evaluation [1,3] deals with the estimate of the various obstacles interposed between the sensitive device and the space external to the satellite. This shield has to be considered as the sum of all the materials in different layers (hypothesis is assumed that the different layer thicknesses can be added).

A code, whose flow-chart is reported in Fig. 3, has been generated in order to execute this task.

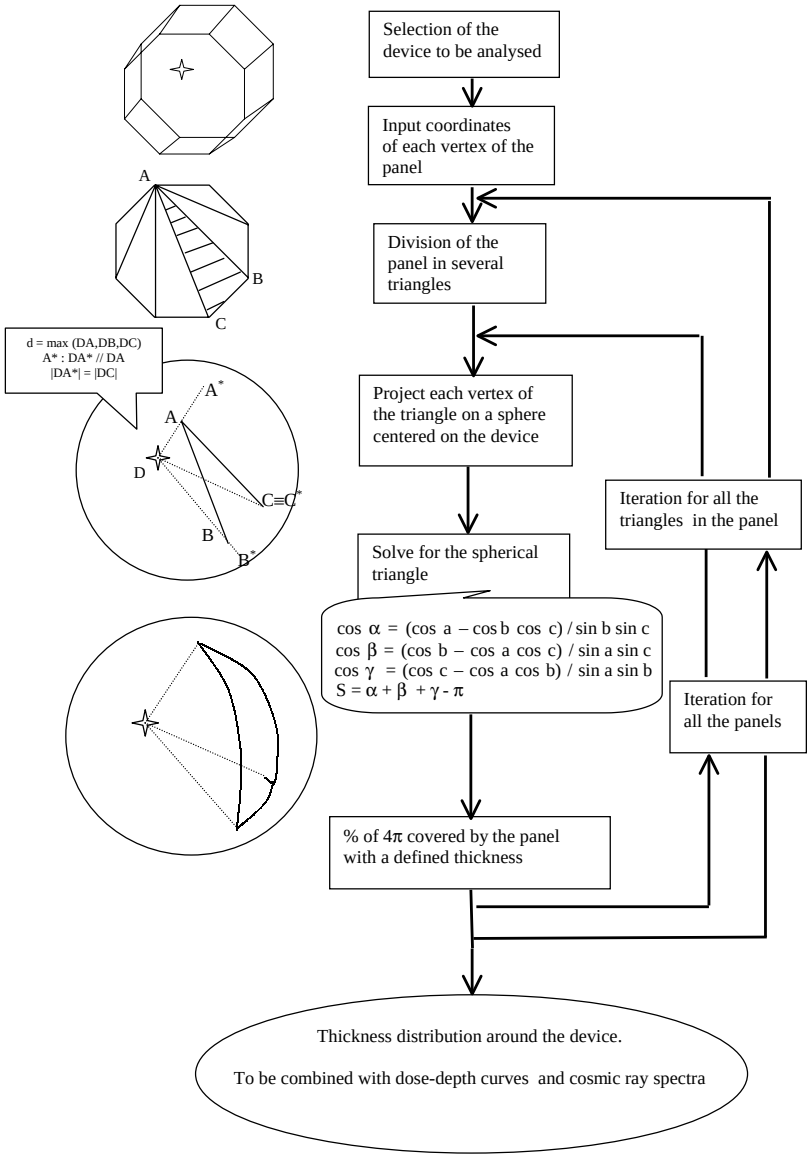


Fig. 3. The procedure implemented to perform the sector analysis.

All the obstacles with a relevant mass interposed between a device and the outside have been considered as panel shields whose thickness is referred to a common standard (mm Al). Their shape is divided into triangular parts. Vertices of each triangle are projected on a sphere, whose radius is normalized with respect to the distance of the point farthest from the device. In such a way, a spherical triangle is obtained, and its surface is easily computed from the coordinates of the vertices. This area is matched, paying attention to the respective thickness, with the shield provided by all the other panels. In such a way, a double column output (Tables 1–3) can be obtained, where the shielding expressed in mm Al is associated with the percentages of 4π-solid angle encompassing the device.

Table 1. Shielding distribution around CPU devices

| CPU/MC 68332 | | CPU/RAM | |
|---|---|---|---|
| mm Al | % | mm Al | % |
| 2.1 | 5.7 | 2.1 | 8.0 |
| 3.2 | 19.8 | 3.2 | 19.6 |
| 4.0 | 4.0 | 4.0 | 5.3 |
| 4.3 | 8.5 | 4.3 | 0.1 |
| 5.1 | 34.9 | 5.1 | 35.0 |
| 6.2 | 11.7 | 6.2 | 17.6 |
| 6.3 | 4.0 | 6.3 | 10.4 |
| 16.0 | 1.5 | 6.0 | 2.0 |
| 22.2 | 7.7 | 22.2 | 2.0 |
| 26.2 | 2.2 | | |

The result is input to the code giving, for a chosen orbit, the amount of radiation actually impinging the device. Proper storage of structure data enables to consider all the device positioning in a

Table 2. Shielding distribution around the multiplexer and the ROM in TNC

| MUX | | ROM TNC | |
|---|---|---|---|
| mm Al | % | mm Al | % |
| 2.1 | 5.1 | 2.1 | 19.3 |
| 3.2 | 23.6 | 3.2 | 3.8 |
| 4.0 | 6.0 | 4.0 | 39.7 |
| 5.1 | 4.3 | 4.3 | 3.2 |
| 6.2 | 17.6 | 5.1 | 0.3 |
| 6.3 | 10.1 | 6.0 | 1.3 |
| 7.1 | 24.1 | 6.2 | 4.9 |
| 17.1 | 7.8 | 7.4 | 6.6 |
| 32.7 | 1.4 | 9.3 | 11.1 |
| | | 16.0 | 1.4 |
| | | 21.1 | 8.4 |

Table 3. Shielding distribution around two points on the payload tray

| Payload 1 | | Payload 2 | |
|---|---|---|---|
| mm Al | % | mm Al | % |
| 1.1 | 22.5 | 1.1 | 20.2 |
| 2.2 | 4.7 | 2.2 | 5.1 |
| 3.0 | 16.3 | 3.0 | 30.1 |
| 5.0 | 9.9 | 3.3 | 3.8 |
| 5.3 | 4.3 | 4.1 | 8.0 |
| 6.1 | 9.1 | 5.2 | 1.4 |
| 6.4 | 8.8 | 6.1 | 8.0 |
| 7.2 | 7.1 | 6.3 | 3.3 |
| 8.3 | 9.1 | 6.4 | 6.8 |
| 15.0 | 1.4 | 7.2 | 4.2 |
| 22.3 | 2.2 | 8.3 | 1.6 |
| 24.3 | 3.6 | 15.0 | 1.9 |
| | | 22.3 | 5.6 |

short time. This procedure is basically a method to assess the shielding more than being an actual design tool. However, a graphical output can be obtained as a chart indicating the most dangerous, less shielded directions. This kind of sketch, that will be shown in the following for the UNISAT case, presents the contour-lines of equally shielded sectors on a sphere centered in the device under study. This process should be repeated for all the devices on board; however, passive components do not require any caution, so the attention can be focussed on some particular active components, such as the MOS technology devices.

### *3.2. Analysis of UNISAT microsatellite*

In the case of UNISAT, several critical components are present. On the communication tray (in the TNC), on the power tray, on telemetry board 3 (with the multiplexer, the current sensors and ADC board), in the OBDH tray (on telemetry boards 1 and 2 and on the SBC board with the MC68332, RAMs and ROMs). The payload tray is considered empty, with respect to the multipurpose concept of UNISAT: an important goal of this research is to evaluate the kind of radiation environment that is to be expected in this section of the satellite, in order to offer some useful information to the payload provider.

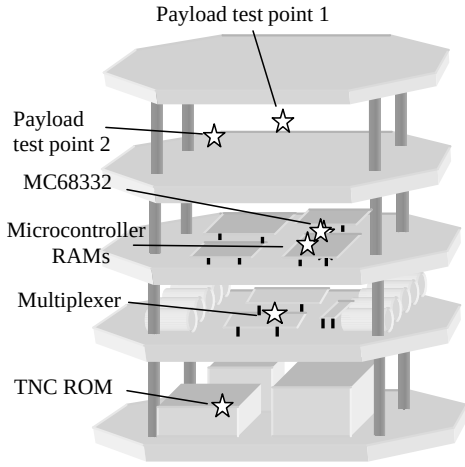


Fig. 4. Position of the devices considered for sector analysis.

The sector analysis presented has to be performed on a selection of devices, which is carried out referring to the two main criteria:

- positioning of test point in order to cover all the volumes of the satellite assessing the relative risk;
- criticality of the device in order to actually determine possible limits of the operational lifetime.

With respect to these criteria, analysis has been limited to the following devices (Fig. 4) [1]: the processor Motorola MC68332, the RAM of the SBC board, the multiplexer Maxim 406 in the telemetry board 3, the ROM TIX TMS27C512 in the TNC, the geometrical center of the payload tray labeled as test point 1, and a position on the same tray about 10 cm from the center, labeled as test point 2.

Shielding thicknesses and their percentages are resumed in the following Tables 1–3.

These thickness distributions can be represented in a graphical form [5]. The curve in Fig. 5 indicates the percentage of $4\pi$ characterized by a shielding thickness less than the value in abscissa (expressed in mm Al).

Critical directions are easily detected by means of a chart obtained as a graphical output of the code devoted to perform sector analysis. Sectors with the same value of equivalent shielding thickness are identified by appropriate contour-lines on the spherical surface encompassing the device. This surface is displayed in a classical 2-D projection with latitude and longitude as coordinates; equatorial plane coincides with the horizontal

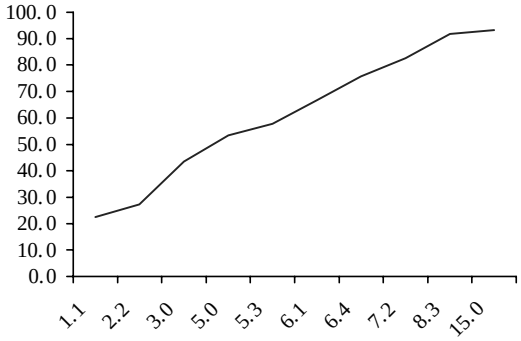


Fig. 5. Graphical representation of the shielding thickness distribution around a device.

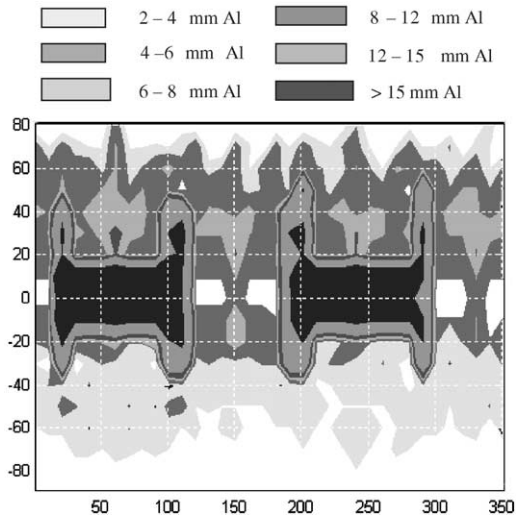


Fig. 6. Graphical representation of the shielding thickness distribution around the multiplexer.

plane containing the device. The projection causes some graphical inaccuracies near the poles of the sphere, but the identification of the "weak" sectors is easily allowed.

Different thickness values for the contour lines can be selected in a case-sensitive way; in the following, we give two examples about the multiplexer on the second shelf and the dose-point "2" in the payload tray. Gray gradation for the contour lines of Figs. 6 and 7. Shielding effect of battery boxes and spacers is apparent for the multiplexer, while the asymmetry of the spacer shielding to dose point "2" marks the distance from the $z$-axis.

#### 4. ENVIRONMENT

The orbit chosen dictates the radiation danger met and the amount of radiation the satellite will have to be protected from.

Unfortunately, the choice of the orbit is not a basic requirement for most of the universitary

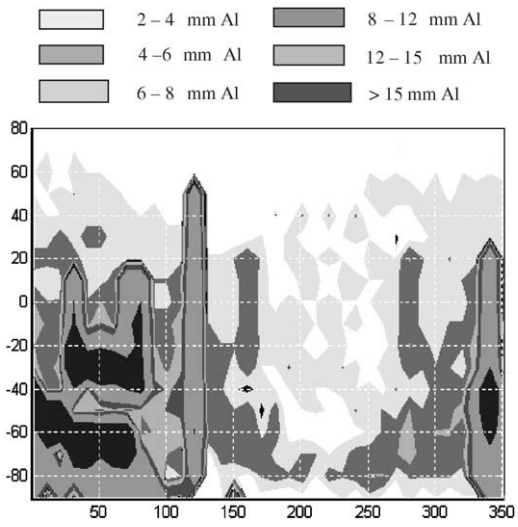


Fig. 7. Graphical representation of the shielding thickness distribution around the point labeled as "payload 2".

microsatellites, as it is strictly dependent on the possibility to have a low or free cost launch as an auxiliary payload, the orbit choice being ruled by the main payload. Indeed, the candidate orbits to be investigated here will be those most commonly used by the launchers: a sunsynchronous, a 51.6° MIR inclination and an equatorial one for the two altitude values of 500 and 800 km.

Dealing with satellites devoted to such a kind of low Earth orbits, a rough description of the radiation environment can be given:

- Trapped particles in the inner (protons from 500 keV to 100 MeV) and outer (electrons up to 7–8 MeV) Van Allen Belt with a spatial distribution encompassing the latitudes between 60°S and 60°N, and with a peak in the correspondence of the South Atlantic Anomaly.
- Solar particles, whose emission is related to the 11-year cycle.
- Cosmic Rays coming from the outer space: very high energy particles ($> 0.1$ GeV) with different $Z$ whose flux is the maximum corresponding to the solar minimum.

The epoch of the launch is quite important in order to define the field strength condition from the set of the extremal values, corresponding to solar minimum, maximum and flare, which will be used for the analysis.

As we will see in the following section, several models are available today to describe this environment [3].

### 5. UNISAT RADIATION ENVIRONMENT

Each orbit of the candidate set for UNISAT mission was evaluated by means of the SPENVIS and CREME96 suites of programs. The former has been used to achieve the dose-depth curves concerning the values of shielding thickness peculiar to the UNISAT structure; the latter has given the cosmic ray fluxes and the attenuation of their effect through the shielding of the satellite.

For each candidate orbit, three different conditions were considered: solar maximum, minimum and flare.

We emphasize here the solar maximum condition, which will characterize next 7 years, taking into account even the occurrence of solar flares.

Data presented are referred to the most risky case, the sunsynchronous orbit at 800 km, where the satellite is directly exposed to the particles coming from sun during solar flares, the protection granted by the geomagnetic field being low at high latitudes. For the same reason, the influence of cosmic rays is effective most too.

Results for the complete set of conditions and orbits are reported in [3].

The TID is mainly given by the trapped protons of the inner Van Allen belt, particularly in the South Atlantic Anomaly; a significant contribution is due to the particles from the Sun and, for small values of shielding thickness, to the trapped electrons. Cosmic rays are negligible for the evaluation of the TID.

In Fig. 8, the dose-depth curves for every source of radiation and the total curve are reported. The dose values refer to the TID collected over the whole scheduled lifetime of the satellite, i.e. one year. We did not consider here the possibility of anomalous large flares which could not be predicted by statistic models. However, this task should be taken into account during the period of solar maximum; Fig. 9 shows the dose-depth curves in the case of occurrence of 2 great solar flares: the increase of the solar particles contribution is quite apparent.

During the solar maximum period, the flux of cosmic rays is minimum, due to the stronger protection given by the solar magnetic field which turns the particles away from the Earth. These particles can be protons or heavier ions, whose number decreases as the atomic number increases.

In the case of solar flares a large amount of such particles comes from the sun for a short time (i.e. a few days): these are the most critical periods for electronic devices aboard the satellite.

Figure 10 shows the spectrum (flux versus energy) of particles having a different atomic number

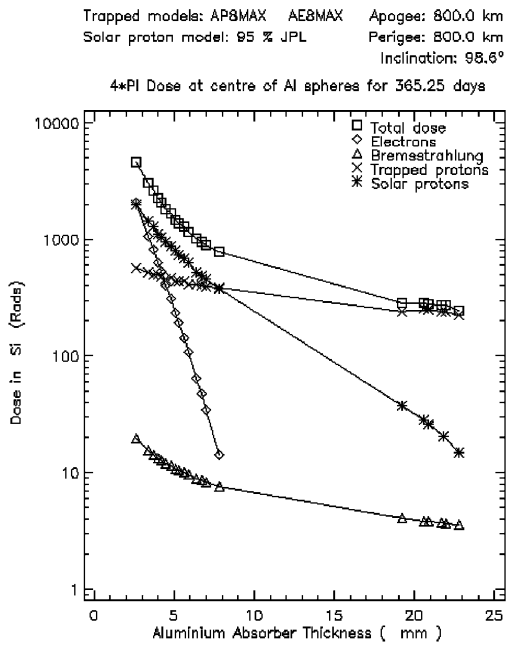


Fig. 8. Dose-depth curves showing the TID collected in 1 year along the 800 km-sunsynchronous orbit (from SPENVIS software).

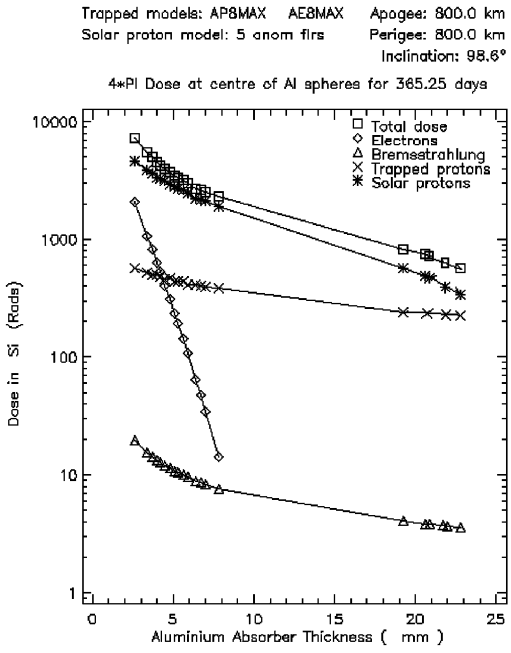


Fig. 9. Dose-depth curves in the case of anomalous solar flares (from SPENVIS software).

$Z$ during a quiet minimum solar period for sunsynchronous 800 km orbit.

In Fig. 11 the same spectrum is pictured in the case of solar flare: the fluxes of particles are much more intense than the previous ones.

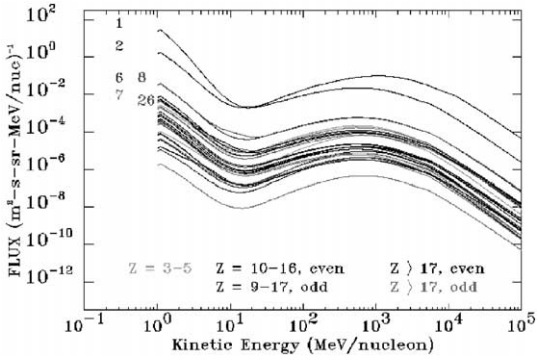


Fig. 10. Cosmic ray spectrum for solar maximum; sunsynchronous orbit at 800 km (CREME96 software).

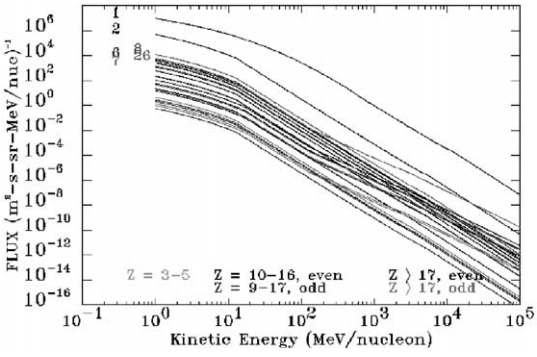


Fig. 11. GCR spectrum in the case of solar flare (CREME96 software).

## 6. TID RESULTS

Combination of environment data regarding each candidate orbit with the geometry-dependent shielding distribution previously evaluated, gives the following results for the total amount of radiation dose throughout the 1 year period. Data are presented with respect to 800 km altitude, circular orbit, with inclinations 51.6° and 98.6° for the solar maximum and in case of larger solar flare (anomalously strong events like those that occurred in 1972 and 1989). Results concerned with Equatorial 800 km orbit, which is not directly affected by solar activity, are also included.

The values are expressed in rad(Si) (Table 4) and indicate the expected doses collected by each device throughout the 1 year lifetime of the satellite. Tantalum (Ta) shielding is also considered for two devices: a strong reduction in the value of annual dose is apparent.

## 7. SEE

Design of the protection against SEE must be carried out on a different basis.

In fact, most of the SEE are brought about by high-energy particles (above 30 MeV); protection given by the surrounding material is effective only on low-energy particles (up to 10 MeV), which are responsible for a small percentage of SEE. Higher-energy protons and ions can not be effectively stopped by interposing shielding material, so alternative methods such as EDAC units or redundant devices must be considered.

It is possible, however, to evaluate the effect of shielding distribution around the devices under consideration. For example, we can see the attenuation of the cosmic ray spectra at the CPU position (Figs. 12–13), which is apparent with respect to the external environment of Figs. 10 and 11.

These spectra have been obtained by means of the CREME96 code using as an input the double-column shaped distribution given by Tables 1–3.

The SEE occurrence is worked out by the same CREME96 code on the basis of the internal spectra and the characteristics of the particular devices under study (sensitive volume, critical charge parameters [2,5]). Daily SEE occurrences on some devices for the most critical orbit condition are presented (Table 5). Experimental data are requested on the specific device under study for the SEE occurrence prediction. Unfortunately, these are not available in every case, but it is often possible

Table 4. Expected doses collected throughout 1 year by different devices. Values are expressed in rad(Si)

| Device | $i = 98.6^\circ$ | | $i = 51.6^\circ$ | | $i = 0^\circ$ |
|---|---|---|---|---|---|
| | flares | max | flares | Max | max |
| Payload 1 | 6878 | 3116 | 3147 | 2825 | 120 |
| Payload 2 | 7206 | 3198 | 3258 | 2909 | 123 |
| CPU/MC | 4180 | 1093 | 1467 | 1198 | 122 |
| " " (Ta) | 1335 | 292 | 510 | 420 | 95 |
| CPU/ROM | 4185 | 1120 | 1471 | 1204 | 115 |
| MUX | 3682 | 984 | 1311 | 1077 | 110 |
| TNC/ROM | 4516 | 1431 | 1718 | 1449 | 115 |
| " " (Ta) | 1500 | 324 | 572 | 470 | 100 |

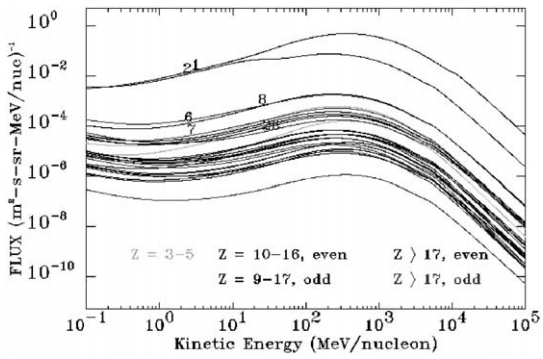


Fig. 12. Cosmic rays spectrum at the CPU position for the sunsynchronous orbit in the case of solar minimum.

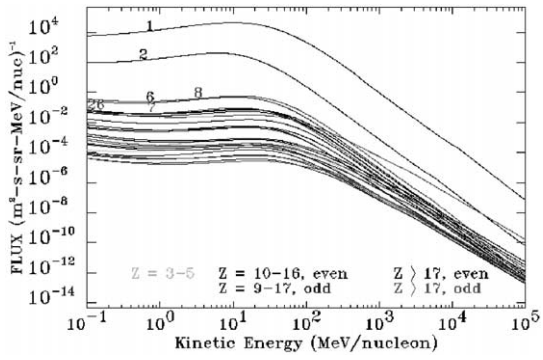


Fig. 13. Cosmic rays spectrum at the CPU position for the sunsynchronous orbit in the case of anomalous flares.

to refer to similar SEE-tested devices (as the MC68020 for the MC68332).

### 7.1. *Spot shielding*

Risk of SEE occurrence resulting from previous results can be considered too high. A possible, moderate help can be provided from the spot shielding [1], i.e. the positioning, of a thick layer just over and under the particular device. Candidate ICs for this application are the most critical components, i.e. the ROM of the TNC and of the SBC 332 board. The layer is made of high density materials, as the tantalum: in the present example, a 2 mm Ta layer is supposed to be placed over the device, which in turn lies on a 1 mm thick Ta layer. In Table 6, the SEE occurrences are resumed for the same devices seen before in such a condition.

Even though the effect of this kind of shielding is not negligible, the method is not completely satisfactory, not being able to reduce the SEE occurrence under values to be considered safe for all the mission lifetime. For some particular device, to be flown in specific orbits, designers are therefore urged to pursue a protection strategy from both hardware and software points of view.

Table 5. Daily SEE occurrence for the more critical devices

| Device | SEE Occurrence |
|---|---|
| MC68332 | 0.0258 events/day |
| ROM TNC | 0.0135 events/day |

Table 6. SEE daily occurrence for tantalum spot-shielded devices

| Device | SEE Occurrence |
|---|---|
| MC68332 | 0.0209 #/day |
| ROM TNC | 0.0095 #/day |

## 8. CONCLUDING REMARKS

A method to evaluate the shielding to radiation offered by the structure has been implemented for the UNISAT microsatellite. The procedure starts with the selection of representative devices, based on their criticality and position on board. Sector analysis is carried out, obtaining by trigonometry the shield distribution. Using up-to-date codes (SPENVIS and CREME96) the dose-depth curves have been generated. The results obtained for the devices onboard show that TID is not expected to cause problems, while the SEE behavior could bring about some trouble for particular devices. A graphical representation of the sector analysis data can be useful in order to qualitatively recognize most dangerous, too weakly shielded directions. The effect of spot shielding via Tantalum lids has been assessed, improving up to $\frac{1}{3}$ the mean time between SEE occurrences.

The analysis presented provides a suitable, general path to investigate and reduce radiation effects on microsatellites.

## REFERENCES

1. The Radiation Design Handbook, ESA PSS-01-609, Issue 1, May 1993.
2. Tylka, A., Private communication.
3. Pizzirani, F., *Criteri di Progetto per la Schermatura di un Microsatellite contro le Radiazioni Spaziali*, Aerospace Engineering Thesis, Università di Roma "la Sapienza", 1997.
4. Graziani, F., Teofilatto, P., Santoni, F. and Palmerini, G. B., The Microsatellite Program at Università di Roma Paper IAA-97-IAA.11.1.03, 48th International Astronautical Congress, Torino, Italy, October 1997.
5. Smith, E. C., Effects of realistic satellite shielding on SEE rates. *IEEE Transactions On Nuclear Science*, 1994, **41**(6) 2396–2399.